Routing Aspects of Electric Vehicle Drivers and Their Effects on Network Performance

Shubham Agrawal[1], Hong Zheng[2], Srinivas Peeta[1,*], Amit Kumar[3]
[1] Lyles School of Civil Engineering, Purdue University, West Lafayette, IN 47907, USA
[2] North Central Texas Council of Governments. Arlington, TX 76011, USA
[3] CQGRD, Georgia Institute of Technology, Atlanta, GA 30308, USA

ABSTRACT

This study investigates the routing aspects of battery electric vehicle (BEV) drivers and their effects on the overall traffic network performance. BEVs have unique characteristics such as range limitation, long battery recharging time, and recuperation of energy lost during the deceleration phase if equipped with regenerative braking system (RBS). In addition, the energy consumption rate per unit distance traveled is lower at moderate speed than at higher speed. This raises two interesting questions: (i) whether these characteristics of BEVs will lead to different route selection compared to conventional internal combustion engine vehicles (ICEVs), and (ii) whether such route selection implications of BEVs will affect the network performance. With the increasing market penetration of BEVs, these questions are becoming more important. This study formulates a multi-class dynamic user equilibrium (MCDUE) model to determine the equilibrium flows for mixed traffic consisting of BEVs and ICEVs. A simulation-based solution procedure is proposed for the MCDUE model. In the MCDUE model, BEVs select routes to minimize the generalized cost which includes route travel time, energy related costs and range anxiety cost, and ICEVs to minimize route travel time. Results from numerical experiments illustrate that BEV drivers select routes with lower speed to conserve and recuperate battery energy while ICEV drivers select shortest travel time routes. They also illustrate that the differences in route choice behavior of BEV and ICEV drivers can synergistically lead to reduction in total travel time and the network performance towards system optimum under certain conditions.

Keywords: Electric vehicles, Route choice behavior, Range anxiety, Multi-class DUE problem, Network performance, Sensitivity analysis

1. Introduction

1.1. *Background and Motivation*

Electric vehicles have received considerable attention in the recent past with the promise of achieving reduced petroleum dependency, enhanced energy efficiency, and improved environmental sustainability. An electric vehicle (EV) uses a battery-powered electric motor for propulsion unlike an internal combustion engine vehicle (ICEV) which is powered by burning gasoline or diesel. Although the environmental sustainability of EVs is debated for the source of electricity generated for recharging the EV's battery, they have a clear advantage over ICEVs due to their efficiency. According to the U.S. Department of Energy (USDOE, 2014), it is estimated that only about 17–21% of the energy stored in the gas tank of an ICEV is converted to power at

* Corresponding author. Tel.: +1-765-494-2209; fax: +1-765-807-3123. E-mail address: peeta@purdue.edu

the wheels. The combustion engine alone loses 62.4% of the energy from fuel as heat. By contrast, EVs convert about 59–62% of the electrical energy from the grid to power at the wheels.

There are two main types of EVs in the market: plug-in hybrid electric vehicle (PHEV) and battery electric vehicle (BEV). PHEVs are equipped with both internal combustion engine and electric motor, and BEVs are equipped with only the electric motor. As a PHEV uses two drive-trains, typically its operating cost is higher than that of a BEV which uses single drive-train. There are unique characteristics currently associated with BEVs, including limited battery capacity and long recharging time that can be limiting for travel compared to ICEVs. Given the current battery technologies, a BEV typically has a driving range of around 80 – 100 miles with a full charge, depending on the vehicle type and battery size. Some premium BEVs, such Tesla Model S, have a higher range of about 250 – 350 miles with the advancement of battery technology which is expected to improve further; however, they are significantly more expensive compared to typical EVs. The limited driving range of BEVs imposes an issue, known as the range anxiety, that is, the driver concerns that the vehicle will run out of battery power before reaching the destination (Tate, et al., 2008). This issue is especially limiting for long trips where the travel distance is close to or beyond the driving range (Mock, et al., 2010; Yu, et al., 2011). This study focuses on BEVs rather than PHEVs as the purpose of this study is to capture range anxiety which is not applicable to PHEVs. A PHEV is similar to a BEV when operating on battery (if range anxiety is not a concern) and an ICEV when operating on gasoline or diesel.

Typically, a BEV spends 6-8 hours (slow charging) to get fully charged, depending on the electrical charging equipment, charging schemes, and battery capacity (Botsford and Szczepanek, 2009). Fast charging technology is available, with 10 minutes charging for a range up to 100 miles. However, it requires special equipment in the power connector and is sparsely deployed in the public infrastructure. Even the “quick charge” facility available at public charging stations can take around 30 minutes to charge the battery up to 80% (USDOE, 2015). Furthermore, fast charging, including quick charging, can deteriorate the battery health and is not advisable on a regular basis (Rezvanizaniani, et al., 2014). Another alternative to en route charging for long distance travel is battery swapping stations (BSS) where a depleted battery pack is quickly swapped with a recharged one. The success of BSS requires car manufacturers to follow certain battery standards, and even then can entail battery stock problem, especially in urban areas. These technological and logistical challenges make BSS impractical to implement (Senart, et al., 2010). Therefore, BEV drivers currently, and in the near future, are expected to charge their vehicles through home-based overnight charging or workplace-based charging mechanisms most of the time.

The market share of EVs has increased significantly in recent years (Mock and Yang, 2014) and is likely to increase further in future, due to multiple incentives such as government subsidies, advancement in battery technology and public acceptance of EVs. Shepherd et al. (2012) investigate the effect of multiple factors such as subsidy, average vehicle life and emission rates on the market penetration of BEVs. Becker and Sidhu (2009) predict that EVs, including both PHEVs and BEVs, could comprise 24% of the light-vehicle fleet in USA by 2030.

The increase in the market penetration of EVs, especially BEVs, will impact the traffic stream, which may imply new driving and route choice imperatives. BEVs are typically equipped with regenerative braking system (RBS) that can recuperate a part of the kinetic energy lost during the deceleration phase to recharge the battery. This is where braking energy that would otherwise be dissipated as heat is captured and restored in the battery. This can increase the driving range of a BEV. Studies show that in typical urban areas, the recuperation could increase range by about 20%, and often more in hilly areas (Artmeier, et al., 2010). Due to the long battery recharging time, en route recharging is usually not an attractive option for BEVs currently, and thus energy-efficient driving and energy recuperation are important factors for BEV drivers. There are two important factors that can encourage a BEV driver to select an energy-efficient route rather than the traditional least travel time route: (i) reduce the operating cost, and (ii) improve the driving range. A BEV driver needs to pay for electricity to charge the battery. In addition, with every charge-discharge cycle, battery life degrades. Therefore, a BEV driver may prefer a route with extra travel time but with reduced energy consumption to decrease operating cost. Because the initial state-of-charge (SOC) of electric battery may not always be full before starting a trip, or the travel distance may be close to the driving range, some BEV drivers may face the dilemma of range anxiety because of the fear of running out of battery charge before completing the trip. In such a situation, a BEV driver may select a route with higher level of congestion to recuperate a part of kinetic energy lost to recharge the battery so as to improve the range. In addition, for BEVs, energy consumed per unit distance traveled is lower at moderate speed than at higher speed. This can further incentivize BEV drivers to select lower speed alternatives under range anxiety. The presence of BEVs in the traffic stream with the above characteristics of route choice raises two interesting questions: (i) whether the incentives in terms of energy savings and range improvement, and the range anxiety factor, can lead to different route selection by BEV drivers as compared to the ICEV drivers, and (ii) whether this difference in route choice behavior can affect network performance in terms of system travel time. These two questions form the motivation for this study.

1.2. *Literature Review*

Past studies related to EVs in the transportation domain can be broadly classified into four groups: EV energy consumption computation, EV energy-efficient routing, EV traffic assignment and facility location of charging stations.

In the context of EV energy consumption computation, electrochemical theory based models require battery-level data like voltage and current while the models using driving parameters such as speed and acceleration generally use basic principles of physics to estimate power consumption. Chan (2000) provides an overview of various electrochemical process based methods. Plett (2004) proposes an extended Kalman-Filtering based method for the battery management system of Lithium-Lead based hybrid EV battery packs. While these methods are essential for battery SOC estimation, it is not practical to use them for the traffic-related perspective here due to their battery data requirements. Battery SOC per unit time can be computed by ADVISOR, a tool developed by the National Renewable Energy Laboratory (NREL) to analyze vehicle performance and fuel economy (Johnson, 2002; Wipke, et al., 1999). It uses basic physics and model component

performance to replicate the vehicle drivetrain process (NREL, 2013). Maia et al. (2011) use a simulator called Simulation of Urban Mobility (SUMO) to simulate the energy consumption of EVs. Wu et al. (2015) use test vehicles installed with an in-vehicle data collection system to measure and analyze EV energy consumption. Tanaka et al. (2008) perform a similar study to determine EV power consumption under different speed profiles. Yao et al. (2013) propose a SOC estimation method based on dynamometer test data. Haaren (2011) analytically compute energy power consumption for EVs and estimate the parameters through curve-fitting based on the Tesla Roadster data published by Straubel (2008). Our study uses the battery model proposed by Haaren (2011) due to its computational efficiency and capability to capture battery recuperation.

Related to energy-efficient routing, Sachenbacher et al. (2011) introduces the problem of finding the most energy-efficient path for EVs with recuperation in a graph-theoretical context. Artmeier et al. (2010) and Storandt (2012) propose revised shortest-path algorithms to address energy-optimal routing. They formulate energy-efficient routing in the presence of rechargeable batteries as a special case of the constrained shortest path problem and propose adaptations of existing shortest path algorithms. Ichimori et al. (1983) and Adler et al. (2014) address the EV shortest-walk problem to determine the route from an origin to a destination with minimum detouring; this route may include cycles for detouring to recharge batteries. Adler and Mirchandani (2014) further study the online routing and scheduling of EVs that involve wait time as well as a reservation scheme to have a fully-charged battery in place due to limited capacity at a battery swap station. Schneider et al. (2014) investigate the EV routing problem with custom time windows and battery-charging stations in a dynamic context. However, they consider the travel time to be independent of flow in the routing model.

In the context of EV traffic assignment, Jiang et al. (2012) formulate a multi-class path constrained traffic assignment model for mixed traffic flow with BEVs and ICEVs. In their model, BEV is a vehicle class with trip length no more than the driving range of full battery capacity, and thus BEVs' equilibrium routes are restricted to the set of distance-constrained paths. However, they do not consider energy recuperation using RBS. Jiang et al. (2014) model the adjustments in combined choices of destination, route and parking for BEVs with a constraint on driving range under equilibrium conditions for mixed traffic flow. Later, Jiang and Xie (2014) extend their model to the combined mode choice and assignment framework by assuming different travel cost functions for BEVs and ICEVs. He et al. (2014) study the network equilibrium of BEVs with recharging capabilities. They propose to minimize the traditional user equilibrium term plus the recharging time. The energy consumption is used to compute the set of usable paths. However, they consider travel time (including recharging time) minimization as the single decision criterion for route choice, and neglect the energy consumption factor in the cost function. In addition, their models focus on static traffic equilibrium rather than dynamic user equilibrium (DUE). Xie and Jiang (2016) propose traffic assignment of BEVs with a relay (node for recharging) requirement. Most traffic assignment related studies assume that the electricity consumption is simply a linear function of the distance traveled and the route travel time (He, et al., 2014; Jiang and Xie, 2014). However, energy consumption is closely related to travel speed, terrain, battery SOC, temperature,

etc. For example, Figure 1 shows the energy consumption rate versus speed for the Tesla Roadster as presented by Haaren (2011).

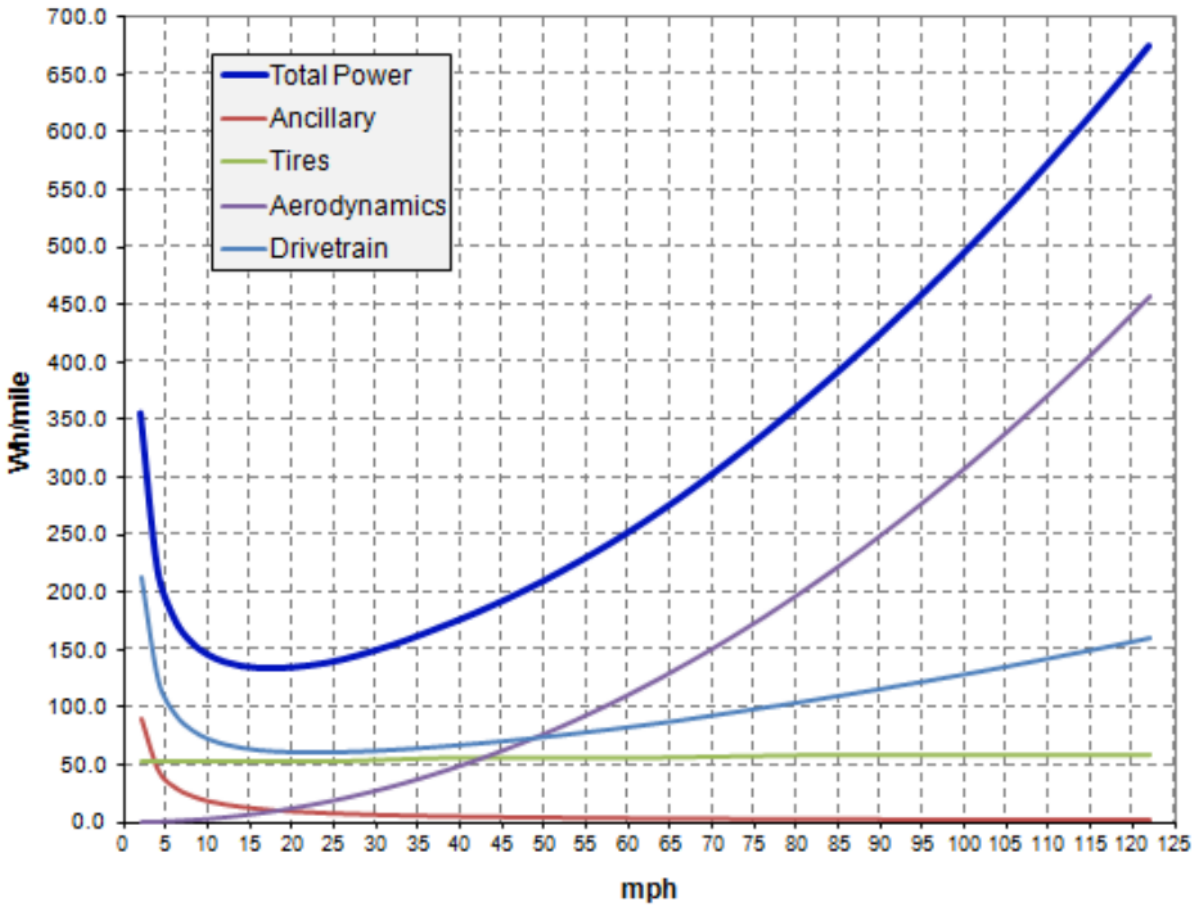

Figure 1 Tesla Roadster Energy Consumption in Watt-hour per mile (Haaren, 2011)

Several studies have investigated the facility location problem of charging stations (Chen, et al., 2013; He, et al., 2013; Hess, et al., 2012; Xi, et al., 2013) and battery-swapping stations (Mak, et al., 2013) where depleted batteries can be recharged or exchanged en route on long trips. Nie and Ghamami (2013) analyze the selection of battery size and charging capacity to meet a given level of service such that social cost is minimized. He et al. (2013) investigate the charging station location problem for PHEVs. The assumption is that PHEVs are always charged at trip destinations, and that travelers jointly select routes and destinations based upon charging prices at destinations. Note that range limitation is not an issue just for BEVs, but also applies to vehicles with alternative fuels which need to find refueling facilities to successfully complete the trip. Several studies have addressed refueling facility location for alternative fuel based trips (Kuby and Lim, 2005; Upchurch, et al., 2009; Wang and Lin, 2009).

In summary, past studies related to travel routing have focused on energy efficient routing decision (Sachenbacher, et al., 2011) and the static user equilibrium assignment subject to range constraint (He, et al., 2014; Jiang, et al., 2012). In these studies, energy consumption is either an exogenous link attribute (Sachenbacher, et al., 2011) or a simple linear function of distance (He,

et al., 2014) and/or travel time (Jiang and Xie, 2014). In reality, a BEV's energy consumption and recuperation are closely related to its drive cycle. A drive cycle is the time series of a vehicle's speed. However, BEV route selection accounting for recuperation capability at the drive cycle level has not been investigated in the assignment context in the literature. Furthermore, the combined effect of energy-efficiency, range anxiety and range improvement in BEV route selection, and the consequent effect on network performance has not been investigated in the past. This study endeavors to bridge these gaps in the literature.

1.3. *Study Significance and Contributions*

This study evaluates the network performance under equilibrium conditions for mixed traffic flow with BEVs and ICEVs by accounting for the difference in their route choice behavior. A multi-class dynamic user equilibrium (MCDUE) model is proposed to investigate the equilibrium of traffic network. The BEVs' route choice behavior is modeled by considering the tradeoff between travel time and energy consumption, and the range anxiety. A microscopic simulation-based solution procedure is proposed to enable accurate computation of energy consumption by using a detailed drive cycle rather than a simple function of distance. The effect of battery recuperation is also factored in estimating energy consumption. Thus, the effect of traffic conditions on energy consumption, and subsequently the route choice of BEVs, is captured in a realistic manner. BEV range anxiety is modeled as a step function that triggers when the remaining battery SOC is less than a pre-specified threshold percentage. This introduces nonlinearity in the travel cost function. As part of the solution procedure, a time-dependent least cost path problem for BEVs is developed as a mixed integer linear model by considering a nonlinear travel cost function.

The study experiments show that ICEVs prefer to choose routes with least travel time while BEVs desire routes with slower speeds to save energy and/or improve range. Based on the current and near future prospects of technology, BEVs will have maximum fuel-efficiency at lower speeds (~15mph) while ICEVs are fuel-efficient in moderate speed range (~45mph). Due to the need for energy-efficiency and range improvement in the route selection for BEVs, the network performance in terms of average travel time and average battery SOC consumption (energy consumption as a percentage of battery capacity) is also analyzed.

This study has contributions for both theory and practice. In a theoretical context, it provides an analytical treatment where the congestion and energy imperatives of ICEVs and BEVs, respectively, are synergistically traded off. This potentially has the synergistic implication that the traffic system performance can be enhanced beyond that of a traffic stream with only ICEVs. This study also extends the current literature related to BEV routing by incorporating the effect of range anxiety in route choice behavior realistically by considering accurate battery SOC consumption based on detailed drive cycle rather than a simple function of distance. From a practical perspective, this result provides insights to decision-makers on analyzing BEV route choice to manage network-wide traffic conditions towards system optimum without exclusively using just monetary instruments like tolling or congestion pricing, at least under mixed traffic environments.

The remainder of the paper is organized as follows. Section 2 discusses the notation used and describes the proposed MCDUE model. Section 3 discusses the solution procedure and implementation issues. Section 4 summarizes results of numerical experiments and their insights. Section 5 provides concluding comments and some future research directions.

2. Multi-Class Dynamic User Equilibrium Model

2.1. *Problem Statement*

We consider a mixed traffic scenario consisting of BEV and ICEV drivers whose route choices are based on the DUE principle with respect to the generalized cost. That is, they seek the individual least time-dependent generalized cost in their route selection. The generalized cost for BEVs includes three components: (1) route travel time, (2) energy consumption, and (3) cost reflecting range anxiety when the remaining SOC level is below a certain threshold. The generalized cost for ICEVs includes only the route travel time. Different from the more extensively studied analytical single user class DUE (Peeta and Ziliaskopoulos, 2001), the problem is modeled as a multiple user class DUE formulation with two vehicle classes (BEVs and ICEVs). This study extends the single user class DUE formulation proposed by Ban et al. (2008) as a complementarity problem to multiple user classes.

Notation

Sets:	
G	Network, $G \equiv (N, A)$;
N	Set of nodes;
A	Set of links;
T	Time horizon;
R	Set of origins;
S	Set of destinations;
$\mathcal{M}$	Set of vehicle classes, $\mathcal{M} \equiv (E, I)$;
E	BEV class;
I	ICEV class;
$A(i)$	Set of outbound links of node $i \in N$;
$B(i)$	Set of inbound links of node $i \in N$;
K_{rs}	Set of simple paths from origin $r \in R$ to destination $s \in S$;
L_k	Sequence of links in path $k \in K_{rs}$.
Indices:	
t	Time period, $t \in T$;
t_d	Departure time period, $t_d \in T$;
i	Node, $i \in N$;
a	Link, $a \in A$;
r	Origin node, $r \in R$;
s	Destination node, $s \in S$;

m	Vehicle class, $m \in \mathcal{M}$;
h_a	Head node of link a;
l_a	Tail node of link a;
k	Path, $k \in K_{rs}$.
Parameters:	
$d_{is}^m(t)$	Time-dependent travel demand from node $i \in N$ to destination $s \in S$ for each vehicle class m in time period $t \in T$
ϑ	Value of time;
α	Coefficient of energy cost for BEV class;
γ	Coefficient of range anxiety cost for BEV class;
ω	Range anxiety threshold percentage;
$\mathcal{K}$	Battery capacity.
Variables:	
$\tau_a(t)$	Travel time on link a in time period t;
$\mathcal{S}_a(t)$	Energy consumed on link a in time period t;
$C_a^m(t)$	Generalized travel cost for vehicle class m on link a in time period t;
$\pi_{is}^m(t)$	Minimum generalized travel cost from node i to destination s for vehicle class m in time period t;
$\tau_a(t)$	Travel time on link a in time period t;
$u_{as}^m(t)$	Inflow rate into link a bound for destination s for vehicle class m in time period t;
$v_{as}^m(t)$	Exit flow rate from link a bound for destination s for vehicle class m in time period t;
$x_{as}^m(t)$	Flow on link a bound for destination s for vehicle class m in time period t;
$u_a^m(t)$	Inflow rate into link a for vehicle class m in time period t;
$v_a^m(t)$	Exit flow rate from link a for vehicle class m in time period t;
$f_{rs,k}^E(t_d)$	Flow on path k from origin r to destination s departing in time period t_d for BEV class;
$\mathcal{S}_T$	Total energy consumption;
β	Variable associated with range anxiety cost; 0 if the total energy consumption ($\mathcal{S}_T$) is less than or equal to range anxiety threshold $\omega * \mathcal{K}$, γ otherwise.

2.2. *MCDUE formulation*

Under DUE, the generalized travel costs of all utilized time-dependent routes for the same departure time are equal and less than or equal to those of unutilized routes. For the MCDUE, this principle holds for each vehicle class. The MCDUE can be formulated as a complementarity problem using Equation (1). The mathematical operator $p \perp q$ denotes that p is perpendicular to q, that is, $p^T q = 0$. Equation (1) implies that for each vehicle class $m \in \mathcal{M}$, the inflow rate $u_{as}^m(t)$ into link a bound for destination s in time period t can be non-zero only if the generalized travel

cost $C_a^m(t)$ on link a in time period t is equal to the difference between the minimum generalized travel cost $\pi_{l_a s}^m(t)$ from tail node l_a of link a to destination s in time period t and the minimum generalized travel cost $\pi_{h_a s}^m\big(t+\tau_a(t)\big)$ from head node h_a of link a to destination s in time period $t+\tau_a(t)$, where $\tau_a(t)$ is the travel time on link a in time period t.

$$0 \le u_{as}^m(t) \perp \left\{C_a^m(t) + \pi_{h_a s}^m\big(t+\tau_a(t)\big) - \pi_{l_a s}^m(t)\right\} \ge 0 \qquad \forall m, a, s, t \qquad (1)$$

Generalized cost functions

As discussed earlier, the generalized travel cost functions are different for the two vehicle classes. For ICEVs, the generalized cost includes travel time only; for BEVs it includes travel time, energy related costs and range anxiety if the remaining battery SOC level is below a threshold. The BEV and ICEV drivers select the least cost routes based on the generalized travel cost. The energy related costs account for both monetary (electricity consumption cost) and non-monetary (such as long-recharging time, battery degradation, etc.) costs related to energy consumption. To incorporate range anxiety behavior, when the remaining SOC is less than a pre-specified threshold percentage (ω) of the battery capacity ($\mathcal{K}$), a cost associated with range anxiety ($\beta = \gamma$) is imposed for the BEV. Otherwise, it is assumed that there is no range anxiety issue for the BEV driver, that is, the range anxiety cost is zero ($\beta = 0$). Also, while the range anxiety threshold can vary across drivers, we assume it to be homogeneous across BEV drivers in both the study formulation and experiments to focus on understanding the network effects of range anxiety by using the notion of low anxiety and high anxiety drivers. Further, the heterogeneity in range anxiety threshold can be seamlessly incorporated by extending the study formulation through the use of multiple BEV classes in the proposed MCDUE.

The generalized travel cost functions for BEVs ($C_a^E(t)$) and ICEVs ($C_a^I(t)$) on link a in time period t are defined using Equations (2) and (3). These cost functions involve two variables, $\tau_a(t)$ and $\mathcal{S}_a(t)$, representing travel time and energy consumption on link a in time period t respectively. The parameters ϑ, α and γ refer to value of time, coefficient of energy related costs and cost associated with range anxiety, respectively.

$$C_a^E(t) = \vartheta \cdot \tau_a(t) + \alpha \cdot \mathcal{S}_a(t) + \beta \cdot \mathcal{S}_a(t) \qquad \forall a, t \qquad (2)$$

$$C_a^I(t) = \vartheta \cdot \tau_a(t) \qquad \forall a, t \qquad (3)$$

$$\beta = \begin{Bmatrix} \gamma & if\ \mathcal{S}_T \ge \omega * \mathcal{K} \\ 0 & otherwise \end{Bmatrix}$$

Mass balance constraints

The mass balance constraints ensure that the flow for each vehicle class m bound for destination s is conserved for every link $a \in A$ in each time period $t \in T$, that is, the rate of change of link

flow $x_{as}^{m}(t)$ is the difference between inflow rate $u_{as}^{m}(t)$ and exit flow rate $v_{as}^{m}(t)$. This constraint is expressed in Equation (4).

$$\frac{dx_{as}^{m}(t)}{dt} = u_{as}^{m}(t) - v_{as}^{m}(t) \qquad \forall m, a, s, t \qquad (4)$$

Flow conservation constraints

These constraints ensure that the flow for each vehicle class m bound for destination s is conserved at every node $i \in N$ in each time period $t \in T$; the total outbound flow from a node is equal to the demand originating at that node ($d_{is}^{m}(t)$) plus the total inbound flow at that node. This constraint is expressed as:

$$\sum_{a \in A(i)} u_{as}^{m}(t) = d_{is}^{m}(t) + \sum_{a \in B(i)} v_{as}^{m}(t) \qquad \forall m, i, s, t \qquad (5)$$

FIFO constraints

The first-in first-out (FIFO) principle states that vehicles departing later cannot, on average, exit a link earlier; that is, vehicles must exit the link later than the vehicles that entered earlier than them. While FIFO may not always hold in reality as vehicles can overtake others, for aggregated flow this constraint is satisfied. FIFO constraints can be represented as:

$$t_1 + \tau_a(t_1) \leq t_2 + \tau_a(t_2) \qquad \forall\, t_1 < t_2 \qquad (6)$$

Flow propagation constraints

The flow propagation constraints describe the spatial and temporal traffic flow dynamics at the macroscopic level (Astarita, 1996) as shown in Equation (7). In particular, these constraints depict the relationship between combined inflow rate in time period t and combined exit flow in time period $t + \tau_a(t)$ of all vehicle classes with change in travel time $\tau_a(t)$ of link a in time period t. These constraints are synergistic with the FIFO principle. They are based on the assumption that driving characteristics, such as maximum speed and acceleration, of all vehicle classes are similar.

$$\sum_{m \in \mathcal{M}} v_{as}^{m}\big(t + \tau_a(t)\big) = \frac{\sum_{m \in \mathcal{M}} u_{as}^{m}(t)}{1 + {d\tau_a(t)}/{dt}} \qquad \forall a, s, t \qquad (7)$$

Definitional constraints

Equation (8) expresses the aggregated inflow rate $u_{a}^{m}(t)$ and exit flow rate $v_{a}^{m}(t)$ over all destinations for link a and vehicle class m in time period t. Equation (9) illustrates the aggregated link flow $x_{a}^{m}(t)$ over all destinations for link a and vehicle class m in time period t. Equations (10) and (11) are the non-negativity constraints for flow and cost variables.

$$u_a^m(t) = \sum_{s \in S} u_{as}^m(t), \qquad v_a^m(t) = \sum_{s \in S} v_{as}^m(t) \qquad \forall m, a, t \qquad (8)$$

$$x_a^m(t) = \sum_{s \in S} x_{as}^m(t) \qquad \forall m, a, t \qquad (9)$$

$$u_{as}^m(t) \geq 0, \qquad v_{as}^m(t) \geq 0, \qquad x_{as}^m(t) \geq 0, \qquad \forall m, a, s, t \qquad (10)$$

$$\pi_{l_{as}}^m(t) \geq 0, \qquad \pi_{h_{as}}^m(t) \geq 0, \qquad \forall m, a, s, t \qquad (11)$$

Feasibility constraints

Feasibility constraints are required to address two issues associated with BEVs: (i) that the trip length does not exceed the BEV battery capacity; (ii) the need to circumvent the possibility of cycles that may arise due to negative link costs for BEVs. We assume that BEV recharging occurs at either origin or destination, and there is no en route charging. Let $f_{rs,k}^E(t_d)$ be the BEV flow on a simple path $k \in K_{rs}$ from origin r to destination s in departure time period t_d. Equation (12) illustrates that the inflow rate $u_{as}^E(t)$ of BEVs on link a bound for destination s in time period t is the sum of flows from all origins $r \in R$ bound for destination s departing in any time period $t_d \in T$ such that these flows reach link a in time period t. Equation (13) defines an indicator variable $I_{a,t}^k(t_d)$ with value equal to 1 if link a is in the sequence of links L_k for path k and the flow departing from origin r to destination s in time period t_d enters link a in time period t, and 0 otherwise. Equations (14) and (15) define a function $\phi_{L_k[j]}(t_d)$ to represent the time period in which the flow departing in time period t_d reaches the j^{th} link in the sequence of links L_k for path k. Note that as variable $\tau_a(t)$ is strictly positive, Equation (15) eliminates the possibility of any cycle in the path. Equation (16) restricts the set of paths K_{rs} to contain paths with minimum generalized cost for every O-D pair rs for every departure time period $t_d \in T$ for BEVs. Equation (17) satisfies the battery capacity constraint for BEVs, that is, the total battery consumption for BEVs on path k from origin r to destination s departing in time period t_d cannot exceed the maximum battery capacity $\mathcal{K}$.

$$u_{as}^E(t) = \sum_{\substack{t_d \in T, \\ t_d \leq t}} \sum_{r \in R} \sum_{k \in K_{rs}} f_{rs,k}^E(t_d) I_{a,t}^k(t_d) \qquad \forall a, s, t \qquad (12)$$

$$I_{a,t}^k(t_d) = \begin{cases} 1 & if\ L_k[j] = a, \phi_{L_k[j]}(t_d) = t \\ 0 & otherwise \end{cases} \qquad \forall j \in I^+, j \leq |L_k| \qquad (13)$$

$$\phi_{L_k[1]}(t_d) = t_d \qquad (14)$$

$$\phi_{L_k[j+1]}(t_d) = \phi_{L_k[j]}(t_d) + \tau_{L_k[j]}\left(\phi_{L_k[j]}(t_d)\right) \tag{15}$$

$$\sum_{j=1}^{|L_k|} C_j^E\left(\phi_{L_k[j]}(t_d)\right) = \pi_{rs}^E(t_d) \qquad \forall r, s, k, t_d \tag{16}$$

$$\sum_{j=1}^{|L_k|} S_a\left(\phi_{L_k[j]}(t_d)\right) \leq \mathcal{K} \qquad \forall r, s, k \tag{17}$$

Equations (1) – (17) constitute the complementarity based MCDUE model. The next section presents a solution procedure for it.

3. Solution Procedure

This section illustrates the solution procedure and summarizes its various components. Analytical methods have been proposed in the literature to solve the complementarity problem (Ban, et al., 2008). The complexity of the MCDUE model is similar to that of the DUE formulation proposed by Ban et al. (2008), and hence a similar solution strategy can be used to solve it analytically.

As discussed earlier, the generalized travel cost function of BEVs consists of travel time, energy consumption, and range anxiety if the SOC level is below a threshold. The energy consumed and its regeneration due to RBS depend on the microscopic drive cycle, particularly the speed and acceleration profiles. These microscopic details of drive cycles, and hence the percentage of battery charge consumed and its regeneration, are difficult to express in an analytical closed form, precluding the use of an analytical solution approach. Therefore, an iterative solution procedure is adopted to solve the MCDUE model. The solution procedure uses a microscopic traffic simulator, an energy consumption model, a time-dependent least cost path algorithm, and a path-flow update mechanism in each iteration.

3.1. *Solution Procedure*

Figure 2 illustrates the steps of the solution procedure. The solution procedure is initialized using a fixed time-dependent origin-destination (O-D) demand for each vehicle class. In the 0th iteration, a set of path flows is determined using all-or-nothing (AON) assignment for each O-D pair for each vehicle class for all time periods. Then, a microscopic traffic simulator (using AIMSUN (Barceló and Casas, 2005; Casas, et al., 2010)) is used for network loading to obtain vehicle travel times and BEV drive cycles based on the initial set of path flows. The energy consumption for BEVs is computed using Haaren's model (Haaren, 2011) based on BEVs drive cycles (see Section 3.3). The energy consumption and travel time for each link in each time period are determined by taking the average of energy consumed and travel time experienced on that link, respectively, for all vehicles entering the link in corresponding time period. Next, the time-dependent least

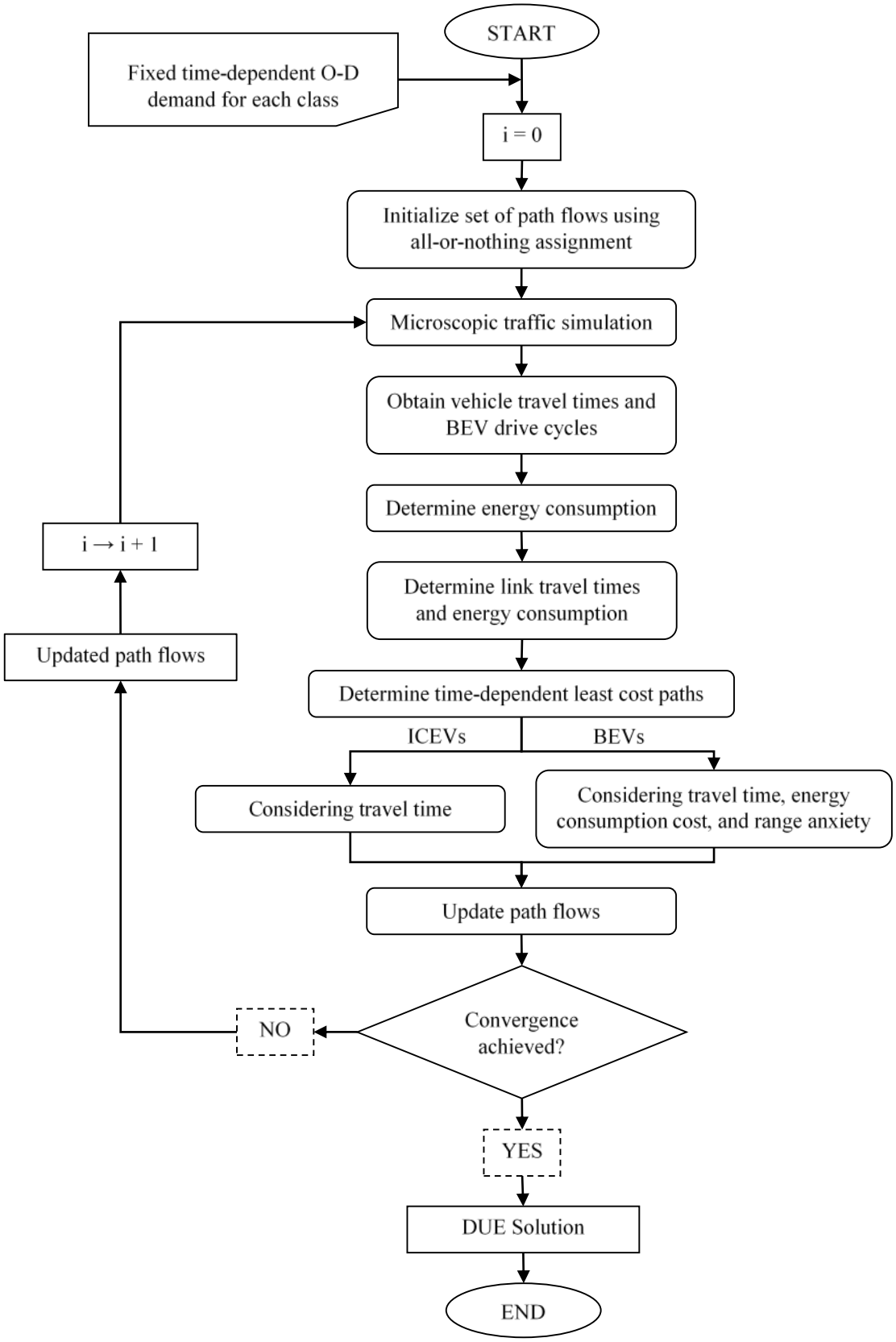

Figure 2 Solution Procedure

(generalized) cost paths (TDLCPs) are determined for both ICEVs and BEVs. For ICEVs, the time, energy related costs and range anxiety. The computed TDLCPs are appended to their corresponding path set if they are already not in that set. The path flows for each O-D pair for each vehicle class for all time periods are updated simultaneously using a modified version of a flow update mechanism proposed by Smith (Smith, 1984). The iteration counter is updated by 1. The updated path flows are simulated using AIMSUN to generate the vehicle travel times and BEV drive cycles. This process is continued until convergence is achieved, which occurs when the average of the difference between the generalized path travel cost of each path of each O-D pair and the lowest generalized path travel cost for that O-D pair is less than 5% of the lowest generalized path travel cost.

3.2. *Role of Microscopic Simulation*

The generalized link travel cost for a BEV includes the battery SOC which requires the vehicle's drive cycle as input to compute energy consumption. Microscopic traffic simulation software AIMSUN is used to obtain link travel times and BEV drive cycles. In zeroth iteration, the simulation is performed using path flows based on AON assignment. In future iterations, the generated TDLCPs and the corresponding flows obtained using the modified Smith's mechanism for both vehicle classes for each O-D pair for all time periods are provided as input to AIMSUN. Hence, the role of microscopic traffic simulation in this study is to generate BEV drive cycles and vehicle travel times.

3.3. *Energy Consumption Model*

The model proposed by Haaren (2011) is used to compute battery energy consumption. It considers power losses at constant speed (V) and variable speed separately. The power loss at constant speed (P_{cons}) is the sum of the losses due to aerodynamics (P_{aer}), drive-train (P_{dr}), rolling resistance (P_{rr}) and ancillary losses (P_{anc}) as shown in Equations (18) to (22). The energy loss at constant speed (E_{cons}) is the summation of power loss over time for the time duration of a vehicle's drive cycle ($\mathcal{D}$). A moving vehicle has two types of kinetic energy (KE): linear (KE_{lin}) and rotational (KE_{rot}). Energy loss at variable speed is due to change in kinetic energy (ΔKE). For computational simplicity, the model assumes that the rotational kinetic energy is about 5% of linear kinetic energy. During acceleration phase, the electric energy is converted into kinetic energy with about 80% efficiency (β_{eff}). During deceleration phase, a part of lost kinetic energy is recuperated as electric energy with efficiency (β_{rbs}) of around 40%. The rate of change of kinetic energy (ΔKE) and the energy conversion from battery-to-wheel and vice versa Thus, the total energy consumption is the net sum of energy losses at constant speed (E_{cons}), energy loss during acceleration phase (E_{acc}) and energy recuperation during deceleration phase (E_{dec}). As stated earlier, the model parameters are based on empirical data from Tesla Roadster, as shown in Table 1. The quality of the model results depends on the time resolution of the drive cycle data (δ); the study experiments use 1-second drive cycle data.

$$P_{aer} = \alpha_{aer} * V^3 \tag{18}$$

$$P_{dr} = \alpha_{dr} * V^3 + \beta_{dr} * V^2 + \gamma_{dr} * V + c_{dr} \tag{19}$$

$$P_{rr} = c_{rr} * N * V \tag{20}$$

$$P_{anc} = 0.2 \tag{21}$$

$$P_{cons} = P_{aer} + P_{dr} + P_{rr} + P_{anc} \tag{22}$$

$$E_{cons} = \sum_{k=1}^{\mathcal{D}/\delta} P_{cons}^{k} * \delta \tag{23}$$

$$KE = KE_{lin} + KE_{rot} \approx 1.05 * KE_{lin} \tag{24}$$

$$KE_{lin} = \frac{1}{2} m V^2 \tag{25}$$

$$E_{acc} = \frac{\Delta KE}{\beta_{eff}} \tag{26}$$

$$E_{dec} = \beta_{rbs} * \Delta KE \tag{27}$$

Table 1 Parameters of the energy consumption model (Haaren, 2011)

Parameters	Value	Parameters	Value
α_{aer}	$3.45 * 10^{-4}$	c_{rr}	0.0075
α_{dr}	$4 * 10^{-6}$	N	7.46
β_{dr}	$5 * 10^{-4}$	β_{eff}	0.8
γ_{dr}	0.0293	β_{rbs}	0.4
c_{dr}	0.375	m	1250

3.4. *Time-Dependent Least Cost Path (TDLCP) Algorithm*

As illustrated in Figure 1, in each iteration the TDLCP algorithm identifies a TDLCP for each vehicle class in each time period for each O-D pair. This path is appended to the corresponding path set if it is not already in it. Flows are shifted from paths with higher generalized costs to those with lower generalized costs (see Section 3.5 for the flow update process).

TDLCPs for BEVs

For BEVs, the generalized cost consists of travel time, energy related costs and the cost associated with range anxiety. The travel time and SOC on each link in each time period are obtained from AIMSUN. To solve the TDLCP problem, we construct a time-expanded network $G^t(N^t, A^t)$ from the original network $G(N, A)$ as follows. For each time period t, a copy of nodes N is created. For each link $a \in A$, if its travel time in time period t is $\tau_a(t)$, a link $b \in A^t$ in time-expanded network connecting from node l_a in time period t to node h_a in time period $t + \tau_a(t)$ is constructed. Thus, the travel time of the newly constructed link (τ_b) is equal to $\tau_a(t)$, and the energy consumed on the newly constructed link $(\mathcal{S}_b)$ is equal to $\mathcal{S}_a(t)$. The TDLCP for BEVs is to find the least generalized cost path in G^t by solving the following mathematical formulation.

Notation

Sets:	
G^t	Time-expanded network;
N^t	Set of nodes in G^t;
A^t	Set of links in G^t;
r^t	Origin node in G^t;
s^t	Destination node in G^t;
Indices:	
b	Link, $b \in A^t$;
Parameters:	
τ_b	Travel time on link $b \in A^t$;
$\mathcal{S}_b$	Energy consumed on link $b \in A^t$;
M	Sufficiently large positive number;
Variables:	
f_{ij}	Decision variable, $f_{ij} \in \{0,1\}$, $f_{ij} = 1$ if link $(i,j) \in A^t$ is selected, 0 otherwise;
y	Auxiliary variable, $y \in \{0,1\}$.

The objective function (28) minimizes the generalized cost that includes three terms: path travel time, energy related costs, and cost associated with range anxiety. Equation (29) is the flow conservation constraint, implying that one unit of flow is sent from source r^t to sink s^t in G^t. Constraint (30) specifies that the energy consumed along the path is bounded by the BEV's battery capacity $\mathcal{K}$, that is, a BEV cannot run out of battery charge en route. Equations (31) – (34) state that if $\sum_{b \in A^t} \mathcal{S}_b \cdot f_b \geq \omega \cdot \mathcal{K}$, then $y = 1$ and $\beta = \gamma$, otherwise $y = 0$ and $\beta = 0$. This implies that the cost associated with range anxiety is triggered only if the battery SOC consumed is more than the specific threshold percentage of battery (ω). If the SOC is below the threshold percentage of battery charge, there is no range anxiety issue for the BEV driver and $\beta = 0$. The parameter M, also known as "big M", allows a binary variable to switch a constraint on or off. In this model, the minimum value of M should be at least $\mathcal{K}$.

$$\min\left(\vartheta \cdot \sum_{b\in A^t} \tau_b \cdot f_b + \alpha \sum_{b\in A^t} \mathcal{S}_b \cdot f_b + \sum_{b\in A^t} \beta \cdot \mathcal{S}_b \cdot f_b\right) \tag{28}$$

$$\sum_{(i,j)\in A^t} f_{ij} - \sum_{(j,i)\in A^t} f_{ji} = \begin{cases} 1 & if\ i = r^t \\ -1 & if\ i = s^t \\ 0 & otherwise \end{cases} \qquad \forall i \in N^t \tag{29}$$

$$\sum_{b\in A^t} \mathcal{S}_b \cdot f_b \le \mathcal{K} \tag{30}$$

$$-M(1-y) \le \sum_{b\in A^t} \mathcal{S}_b \cdot f_b - \omega \cdot \mathcal{K} \le M(y) \tag{31}$$

$$-M(1-y) \le \beta - \gamma \le M(1-y) \tag{32}$$

$$-My \le \beta \le My \tag{33}$$

$$y \in \{0,1\}, f_b \in \{0,1\} \qquad \forall b \in A^t \tag{34}$$

Equations (28) – (34) specify a constrained shortest path problem as a mixed integer formulation. Note that the third term of objective function is nonlinear, which makes the model difficult to solve. Hence, next, we linearize the nonlinear term.

Introduce a dummy variable μ_b such that $\mu_b = \beta \cdot f_b$. Then, the objective function be expressed as Equation (35). The constraint set (36) – (39) indicates that if $f_b = 1,\ \mu_b = \beta$; otherwise $f_b = 0$, then $\mu_b = 0$. Then, the objective function (35) is linear. In summary, Equations (29) – (39) represent a mixed integer linear program (MILP) that is solved to obtain the TDLCPs for the BEV class. The proposed MILP is solved using IBM ILOG CPLEX 12.5 MILP solver (CPLEX, 2015).

$$\min\left(\vartheta \cdot \sum_{b\in A^t} \tau_b \cdot f_b + \alpha \cdot \sum_{b\in A^t} \mathcal{S}_b \cdot f_b + \sum_{b\in A^t} \mu_b \cdot \mathcal{S}_b\right) \tag{35}$$

$$\mu_b \le \beta \qquad \forall b \in A^t \tag{36}$$

$$\mu_b \ge \beta - M(1-f_b) \qquad \forall b \in A^t \tag{37}$$

$$\mu_b \ge 0 \qquad \forall b \in A^t \tag{38}$$

$$\mu_b \le M \cdot f_b \qquad \forall b \in A^t \tag{39}$$

TDLCPs for ICEVs

For ICEVs, the generalized travel cost consists of travel time only. The travel time on each link in each time period is obtained from AIMSUN. Then, the decreasing order of time (DOT) algorithm (Chabini, 1998) is implemented to compute the time-dependent shortest paths. These paths are used to update the path set for ICEVs in each time period for each O-D pair.

3.5. *Path Flow Update Process*

After the TDLCPs are computed in an iteration, they are appended to their corresponding path set and path costs are updated for all paths in the set. The path sets for both vehicle classes for all O-D pairs for each time period are updated simultaneously using the modified Smith's mechanism (Smith, 1984).

Modified Smith's mechanism

Sets:	
W	Set of origin-destination (O-D) pairs;
P_{wt}^{m}	Set of paths for vehicle class m and O-D pair w in time period t
Indices:	
w	O-D pair, $w \in W$;
i, j	Indices for paths, $i, j \in P_{wt}^{m}$;
Variables:	
$C_{wt}^{m}(i)$	Generalized travel cost for vehicle class m and O-D pair w on path i in time period t;
$\Delta C_{wt}^{m}(i,j)$	Generalized travel cost difference between path i and path j for vehicle class m and O-D pair w in time period t;
$\Delta \hat{C}_{wt}^{m}(i,j)$	Normalized cost difference between path i and path j for vehicle class m and O-D pair w in time period t;
f_{wt}^{m}(i)	Flow on path i for vehicle class m and O-D pair w in time period t;
Δf_{wt}^{m}(i)	Change in flow on path i for vehicle class m and O-D pair w in time period t;
f^{*m}_{wt}(i)	Updated flow on path i for vehicle class m and O-D pair w in time period t;

Step 1: For each time period and each O-D pair, compute the difference in generalized cost between each path pair for each vehicle class:

$$\Delta C_{wt}^{m}(i,j) = C_{wt}^{m}(i) - C_{wt}^{m}(j) \qquad \forall m, w, t, i, j \qquad (40)$$

Step 2: Normalize the generalized cost difference using the difference between the maximum and the minimum generalized cost for a vehicle class for each O-D pair and each time period:

$$\Delta\hat{C}_{wt}^{m}(i,j) = \frac{\Delta C_{wt}^{m}(i,j)}{\max_{k\in P_{wt}^{m}}(C_{wt}^{m}(k)) - \min_{k\in P_{wt}^{m}}(C_{wt}^{m}(k))} \qquad \forall m,w,t,i,j \qquad (41)$$

Step 3: Obtain the move direction by summing the inflows and outflows for each path as follows:

$$\Delta f_{wt}^{m}(\mathrm{i}) = \sum_{j,\Delta\hat{C}_{wt}^{m}(i,j)\geq 0} \Delta\hat{C}_{wt}^{m}(i,j) * f_{wt}^{m}(\mathrm{i}) + \sum_{j,\Delta\hat{C}_{wt}^{m}(i,j)<0} \Delta\hat{C}_{wt}^{m}(i,j) * f_{wt}^{m}(\mathrm{j}) \qquad \forall m,w,t,i \qquad (42)$$

Step 4: Simultaneously update the path flows for both vehicle class for all O-D pairs for all time periods using step size α. The step size α is the inverse of the iteration number. Then, the equation for path flow update is as follows:

$$f^{*m}_{wt}(i) = f_{wt}^{m}(i) + \alpha * \Delta f_{wt}^{m}(i) \qquad \forall m,w,t,i \qquad (43)$$

The flow update mechanism presented heretofore is obtained through three important modifications to Smith's flow update mechanism. First, it uses multiple vehicle classes and the temporal dimension to reflect flow propagation of BEVs and ICEVs along various links, unlike the static context of Smith's mechanism where a path flow is considered to be present on all links of that path simultaneously. Second, it normalizes the cost difference (see Equation (36)) before determining the move direction of the flow update process, leading to improved convergence. Third, it updates the path flow vectors for both vehicle classes for all time periods for all O-D pairs simultaneously to eliminate order bias in the flow update process.

4. Numerical Experiments

4.1. *Experiment Setup*

Figure 3 illustrates the network used for the study experiments. It consists of 35 nodes, 68 links, 7 origins/destinations and 42 O-D pairs with non-zero demand. Origins and destinations are marked through A - G. The network has four types of links: freeway, two-lane arterial, one-lane arterial, and ramps. The arterials are connected to the freeway through 12 ramps at three interchanges.

The experiments are conducted for a one-hour horizon of interest preceded by a 15-minute warm-up period. Hence, the time horizon is divided into 75 time periods of 1 minute each. The simulation is allowed to run until all vehicles exit the network beyond the 75-minute horizon. The base O-D demand for the time horizon is presented in Table 2. The demand for each time period is computed by multiplying the base O-D demand with the temporal demand distribution factors shown in Figure 4. The demand for the warm-up period is identical to that of the first time period,

and the demand for the clearance period is zero. The demand for each vehicle class is determined by its market penetration.

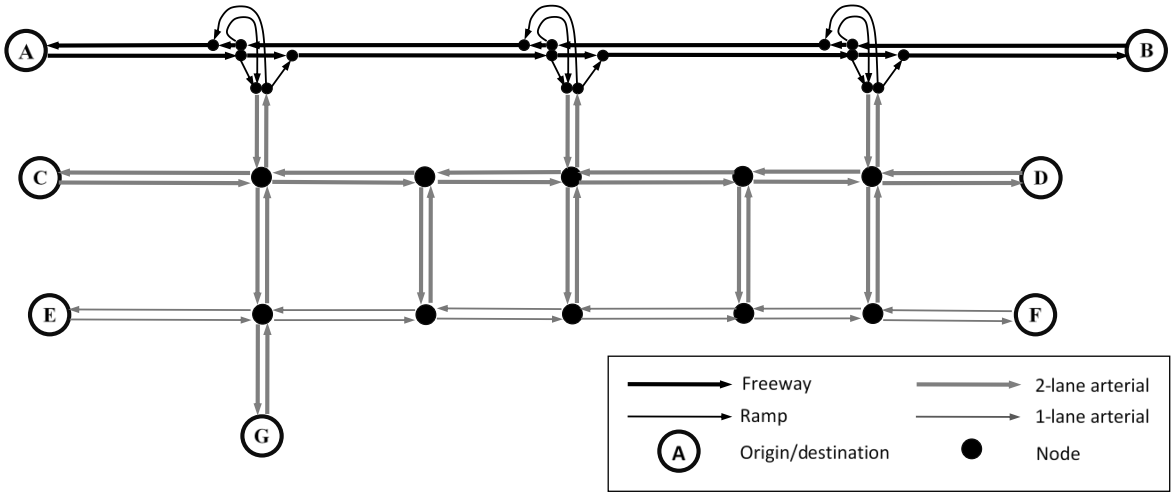

Figure 3 Study Network

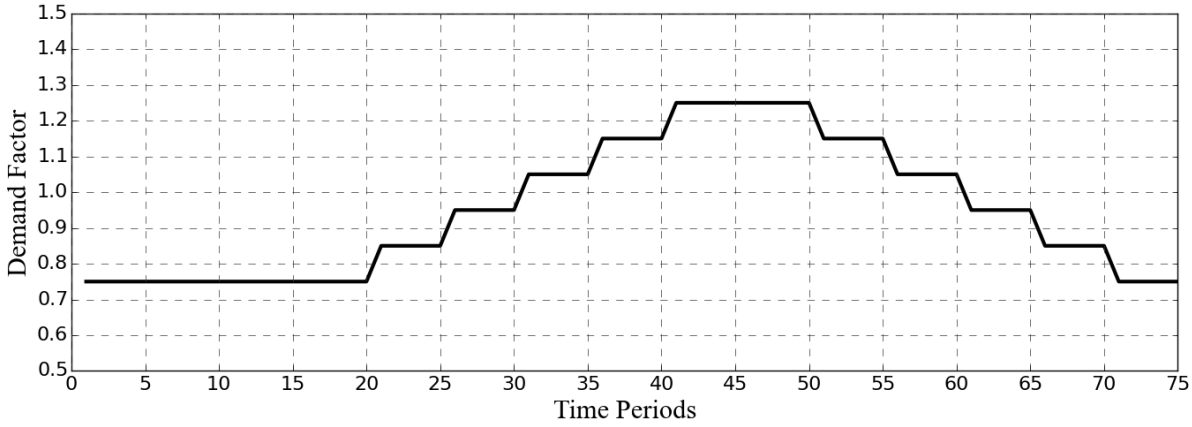

Figure 4 Temporal Distribution of Demand Factors

Table 2 Base Demand for the Time Horizon

O/D	A	B	C	D	E	F	G
A	0	3000	160	250	70	70	100
B	3000	0	375	100	125	50	300
C	75	100	0	100	40	35	75
D	75	50	100	0	50	25	100
E	75	100	40	50	0	50	40
F	75	40	40	25	40	0	40
G	125	150	75	100	100	50	0

The value of travel time for both ICEVs and BEVs is assumed to be $20 per hour. In the numerical experiments, the energy related costs are captured by factoring the non-monetary cost component through an increase in the coefficient value for the electricity consumption cost. The cost of electricity and the BEV range anxiety threshold are varied to perform sensitivity analysis. The effect of the BEV market penetration on network performance is also analyzed.

4.2. *Effect of BEV Market Penetration*

Sensitivity analysis is performed for BEV market penetration under the scenario with no range anxiety. The electricity cost is assumed to be 50 cents/kWh as the fee to recharge a BEV at a commercial level 2 charging station may range between 30 cents/kWh to 80 cents/kWh (Blink, 2015). Figure 5 illustrates the effect of the BEV market penetration on the travel time distribution of BEVs and ICEVs. The average travel time of ICEVs is less than that of BEVs, implying that BEVs trade off their travel time for savings in energy consumption while ICEVs prefer routes with least travel time. Further, the system performance in terms of the total system travel time (TSTT) improves as the market penetration of BEVs increases. This is because as the BEV market penetration increases, more BEVs shift from freeway to arterials, thereby enhancing the performance of freeway as illustrated by Figure 6. Since freeway flows are typically larger than arterial flows, this shift tends to have a positive impact on overall network performance with the BEV market penetration increase. Hence, the preference of some BEVs to choose paths with higher travel time to save battery SOC consumption or recuperate battery charge moves the network towards system optimality in terms of TSTT. Though the total number of vehicles on freeway decreases with increase in BEV market penetration, the number of BEVs on freeway increases leading to the general trend of reduction in BEV average travel time.

While it is expected that an increase in market penetration of BEVs should increase the average travel time of BEVs, the opposite trend is observed in Figure 5. This phenomenon can be explained as follows. As the total travel demand is fixed, an increase in market penetration implies that more BEVs from all O-D pairs shift to arterial routes except for the O-D pairs A-B and B-A (refer Figure 3) for which the freeway still remains the optimal route. Therefore, with an increase in market penetration of BEVs, the overall traffic volume on the freeway decreases. Thus, the average travel time of ICEVs decreases as most of them use the freeway route and its travel time decreases due to the decrease in volume. The average travel times of BEVs for O-D pairs A-B and B-A also decreases as most of them use the freeway route. Since, the travel demand for these two O-D pairs is significantly larger than for the other O-D pairs (refer Table 2), the weighted decrease in travel time of BEVs of these O-D pairs outweighs the weighted increase in travel times of all other O-D pairs. Therefore, an overall decrease in system level average travel time is observed.

The effect of market penetration on the average BEV battery SOC consumption is illustrated in Figure 7. The average battery SOC consumption increases with the increase in market penetration of BEVs because the number of ICEVs decreases, and hence more number of BEVs are present on freeway (see Figure 6). Due to the relatively higher speed on freeway compared to arterials coupled with the fact that higher speed increases energy consumption (see Section 3.3), the average

battery SOC consumption increases as the number of BEVs on freeway increases with market penetration.

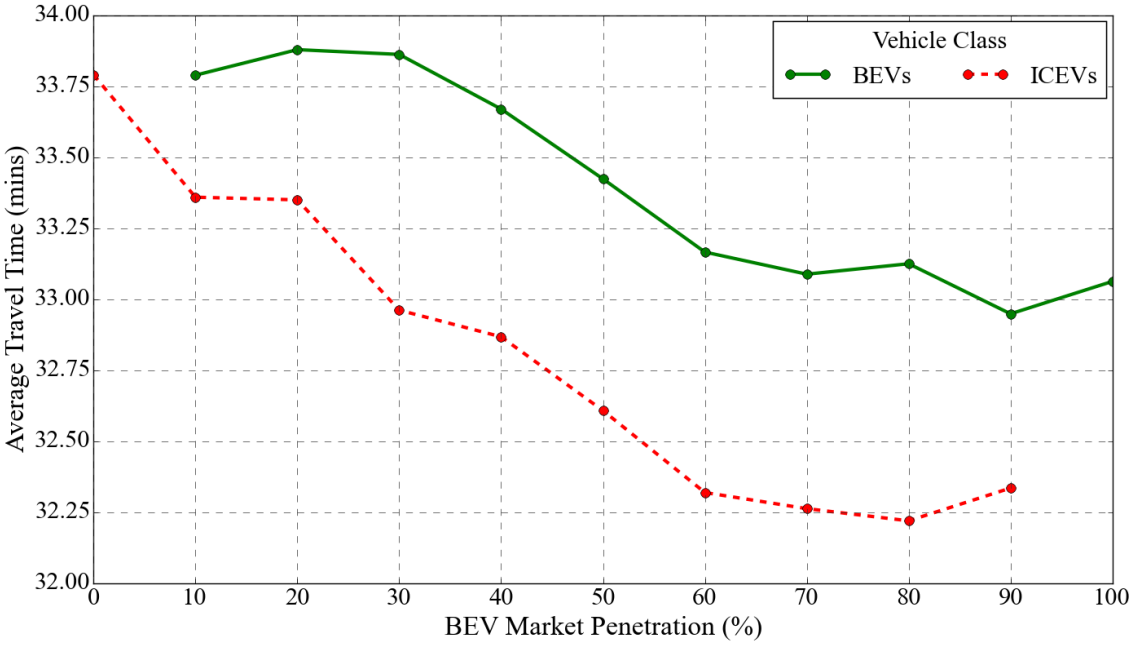

Figure 5 Effect of BEV Market Penetration on Average Travel Time by Vehicle Class

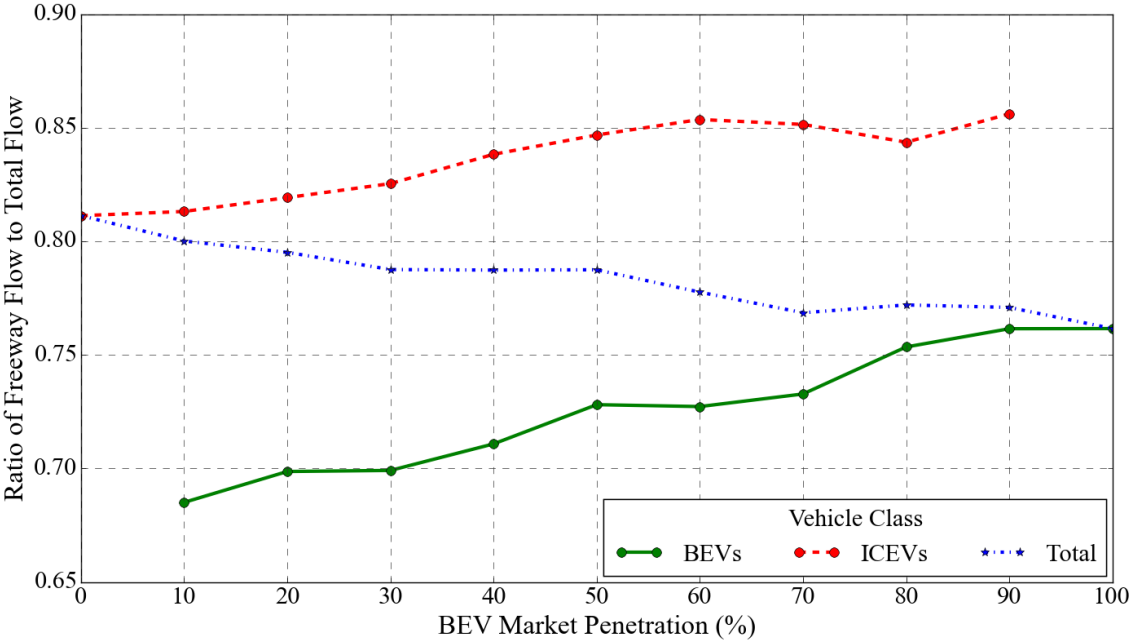

Figure 6 Effect of BEV Market Penetration on Freeway Flows

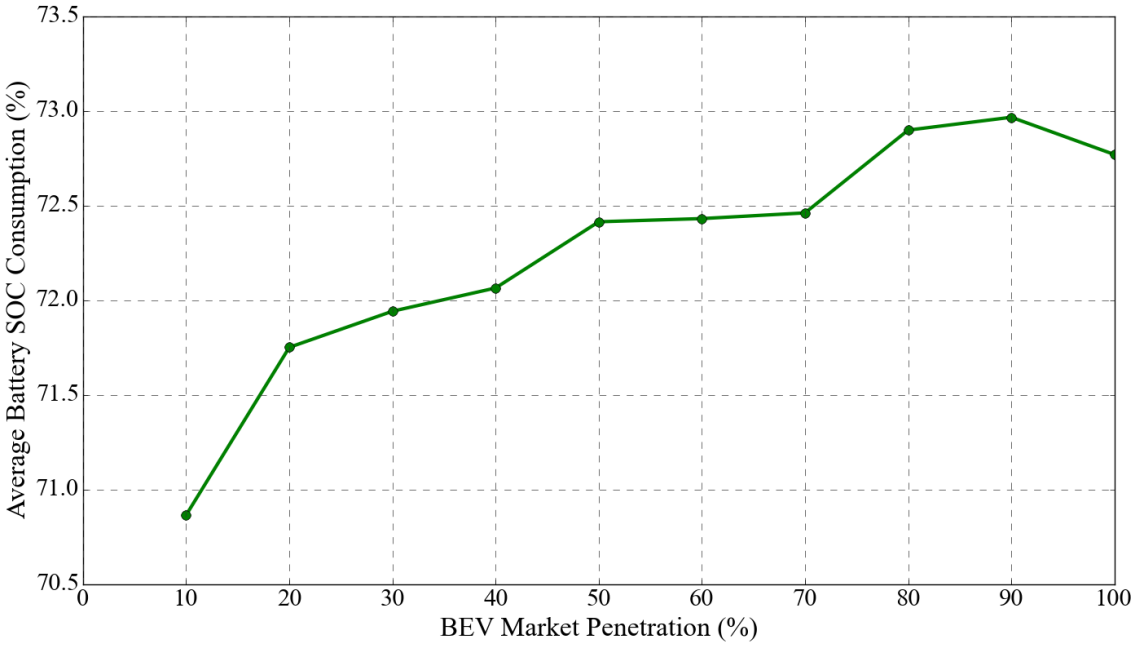

Figure 7 Effect of BEV Market Penetration on Average Battery SOC Consumption

4.3. *Effect of Electricity Cost*

The effect of electricity cost on network performance is analyzed for the case with no range anxiety and equal market penetration of BEVs and ICEVs. Figure 8 shows the relationship between average travel time and electricity cost. The average travel time reduces for ICEVs with an increase in electricity cost, but has an overall negative effect on BEVs. At low electricity costs, the magnitude of positive effect for ICEVs is slightly higher than that for BEVs leading to an overall positive effect for the system. Akin to the discussion in Section 4.2, the increase in average travel time for BEVs and decrease for ICEVs can be explained by the shift in the flow of BEVs from freeway to arterials, as illustrated in Figure 9. At higher electricity costs, more BEVs shift from freeway to arterials as they have more incentive to save on energy consumption though these routes are longer in terms of travel time. This initially leads to a decrease in freeway travel time, thereby causing a decrease in average travel time for both BEVs and ICEVs. At the higher range of electricity costs, a large fraction of BEVs shift to arterials leading to high congestion. While this large shift by BEVs leads to further decrease in average travel time for ICEVs on freeway, the increase in travel time of BEVs on arterials more than negates benefits on freeway and causes system level increases in average travel time. As a result, average travel time of the system increases beyond a certain electricity cost.

The effect of electricity cost on the average battery SOC consumption for BEVs is illustrated in Figure 10, which indicates that the average battery SOC consumption decreases with electricity cost increase. As the electricity cost increases, BEVs have more incentive to shift to routes with lesser battery SOC consumption, and hence more BEVs shift from freeway to arterials (as shown

in Figure 9). Due to the relatively lower speed on arterials compared to freeway, the battery SOC consumption decreases (see Section 3.3).

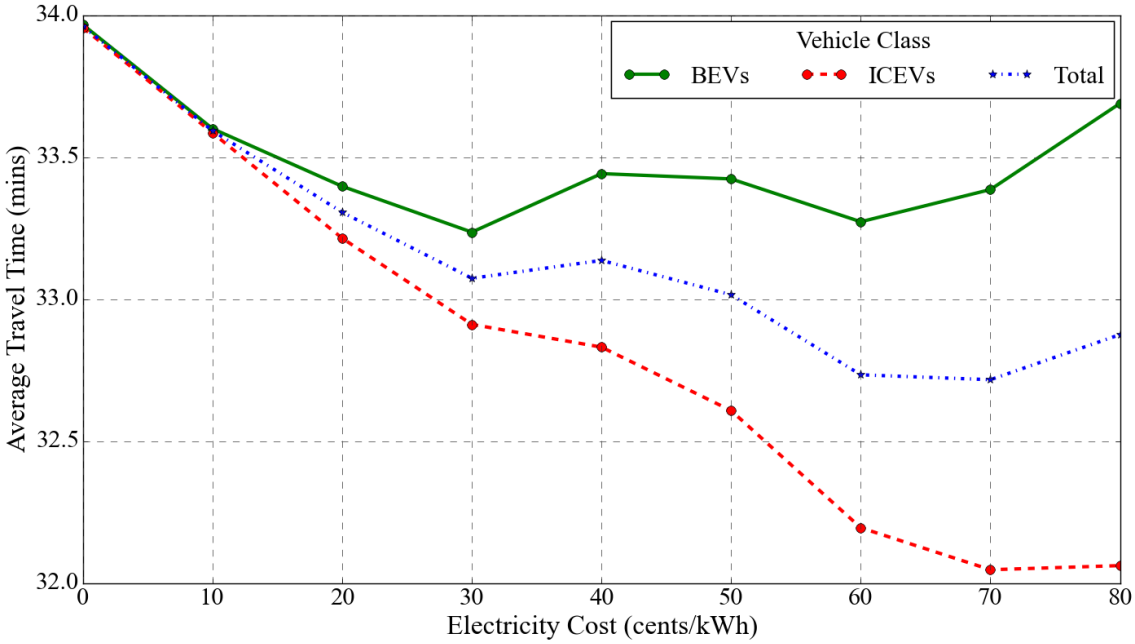

Figure 8 Effect of Electricity Cost on Average Travel Time

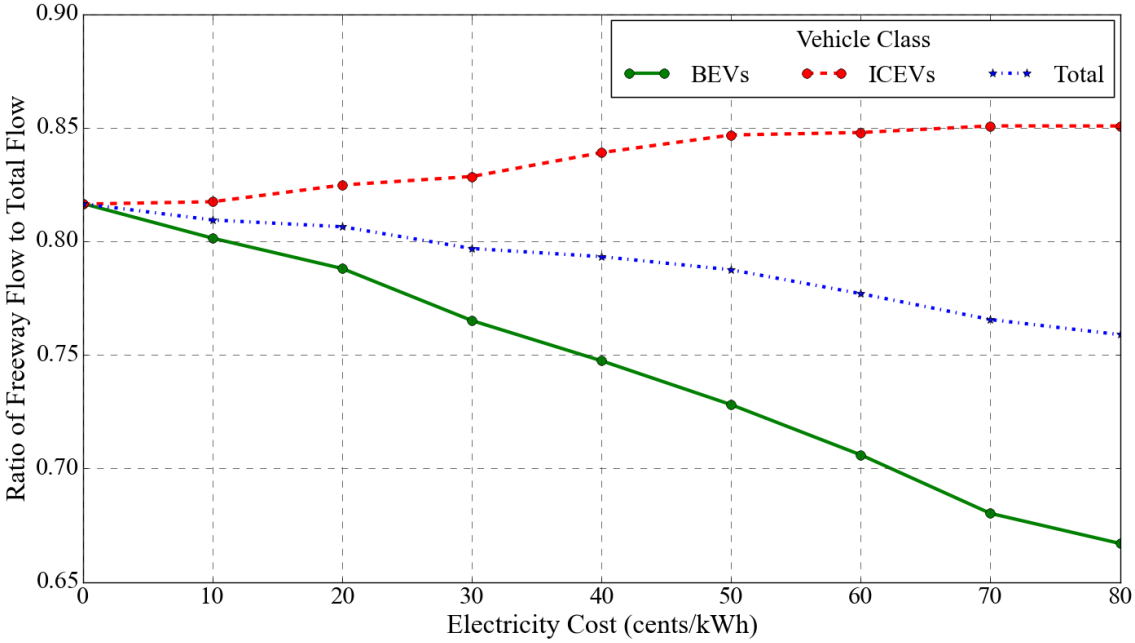

Figure 9 Effect of Electricity Cost on Freeway Flow

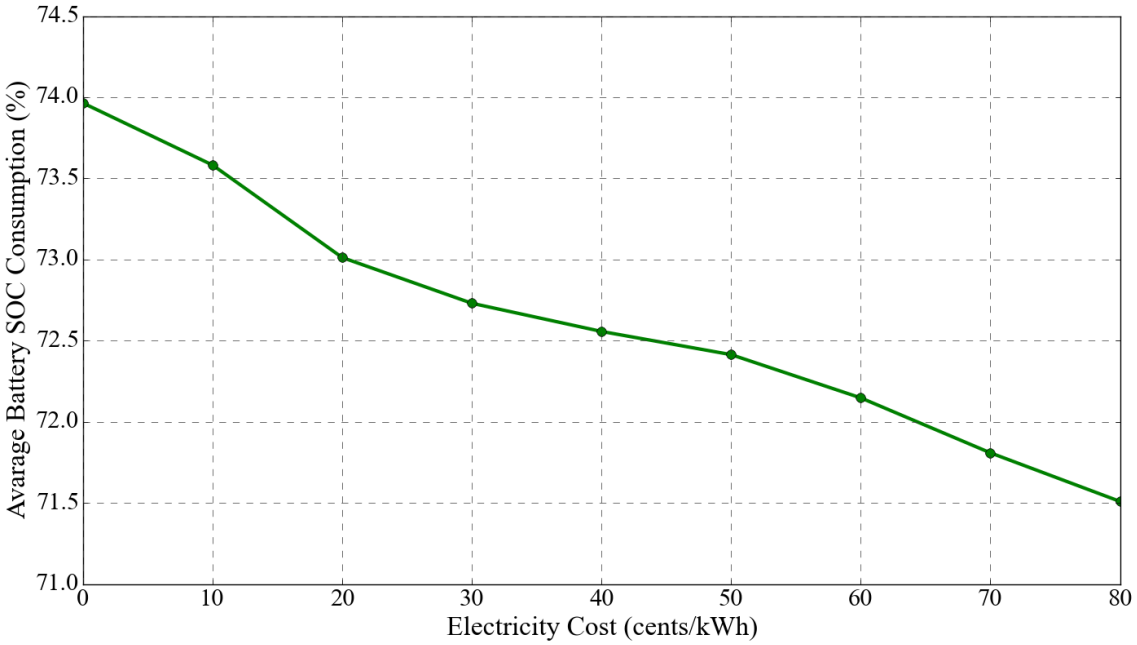

Figure 10 Effect of Electricity Cost on Average Battery SOC Consumption

4.4. *Effect of Range Anxiety*

To analyze the effect of range anxiety, it is classified into low range anxiety and high range anxiety. A driver with high range anxiety is more reluctant towards consuming battery SOC and feels anxious at a relatively higher level of remaining battery capacity compared to a driver with low range anxiety. The typical percentage of battery SOC consumption on the freeway route in the study network is around 75-80%. Hence, high range anxiety is assumed to be triggered when a BEV consumes 70% of the battery capacity (that is, 30% battery is remaining) and low range anxiety is assumed to be triggered when 90% of the battery capacity (that is, 10% battery is remaining) is consumed. Figure 11 illustrates the effect of range anxiety on travel time distribution of BEVs and ICEVs for an electricity cost of 50 cents/kWh and equal market penetration of ICEVs and BEVs. It indicates that high range anxiety has a negative impact on the network performance as BEVs experience higher travel times under high range anxiety compared to the case of low range anxiety. Vehicles with travel time of around 20 minutes in the network are typically those for which destinations are relatively closer to their origins and mostly use arterial routes (see Figure 3). At high range anxiety, a significant number of BEVs use routes with higher travel time to reduce battery SOC consumption and hence shift from freeway to arterial routes. This causes severe congestion on the arterial routes and has a negative impact on the travel time of the vehicles on arterial routes, including vehicles whose trips partly involve arterial travel. Hence, all vehicles including ICEVs experience relatively higher travel times under high range anxiety, with BEVs performing slightly worse than ICEVs, on average.

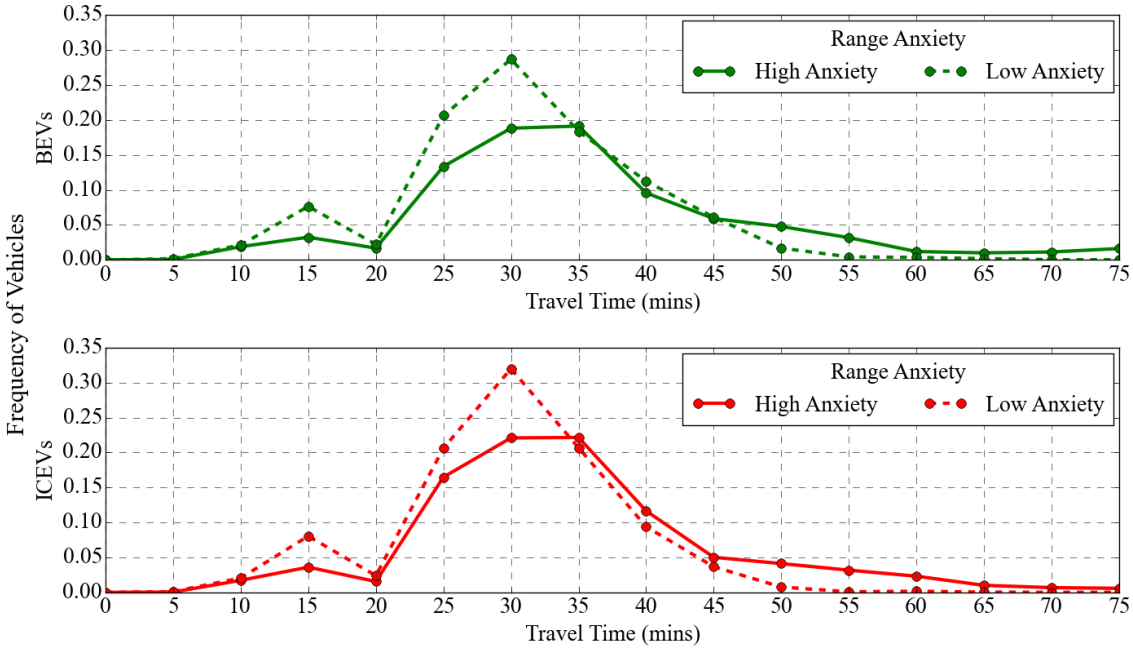

Figure 11 Effect of Range Anxiety on Travel Time Distribution

4.5. *Effect of Congestion Level*

The effect of congestion level on route selection by BEVs is analyzed for the case of equal market penetration, an electricity cost of 50 cents/kWh and without range anxiety. Congestion levels are classified as free flow, mild congestion, moderate congestion and high congestion based on average network speeds of about 50 mph, 31 mph, 21 mph and 15 mph, respectively. Figure 12 shows the ratio of freeway flow to total flow for BEVs and ICEVs. The freeway flow for both ICEVs and BEVs decreases with increase in congestion and the difference between freeway flow of ICEVs and BEVs decreases as well. With increase in congestion, the travel time on freeway route increases, and hence vehicles tend to move to alternative routes. Under free flow, BEVs save on electricity cost by selecting arterial routes as they have slower speeds. As congestion increases, the average speeds on both freeway and arterials decrease, reducing the incentive for BEVs to select arterial routes. Hence, as congestion increases, BEV behavior is closer to that of ICEVs in terms of route selection.

Figure 13 shows the effect of traffic congestion on average battery SOC consumption. The average battery SOC consumption decreases up to the moderate congestion level and then increases slightly for the high traffic congestion level. This can be explained using the relationship between speed and energy consumption per mile for BEVs in Figure 1. The energy-efficiency for BEVs is lowest under free flow as the vehicles consistently drive at high speeds. As congestion increases, the speed decreases, and up to a certain point the average battery SOC consumption also decreases. Under high congestion, though the average network speed is about 15 mph, a good proportion of BEVs travel at very low speeds (less than 10mph) for a major portion of their trip with low energy-efficiency, increasing their average battery SOC consumption.

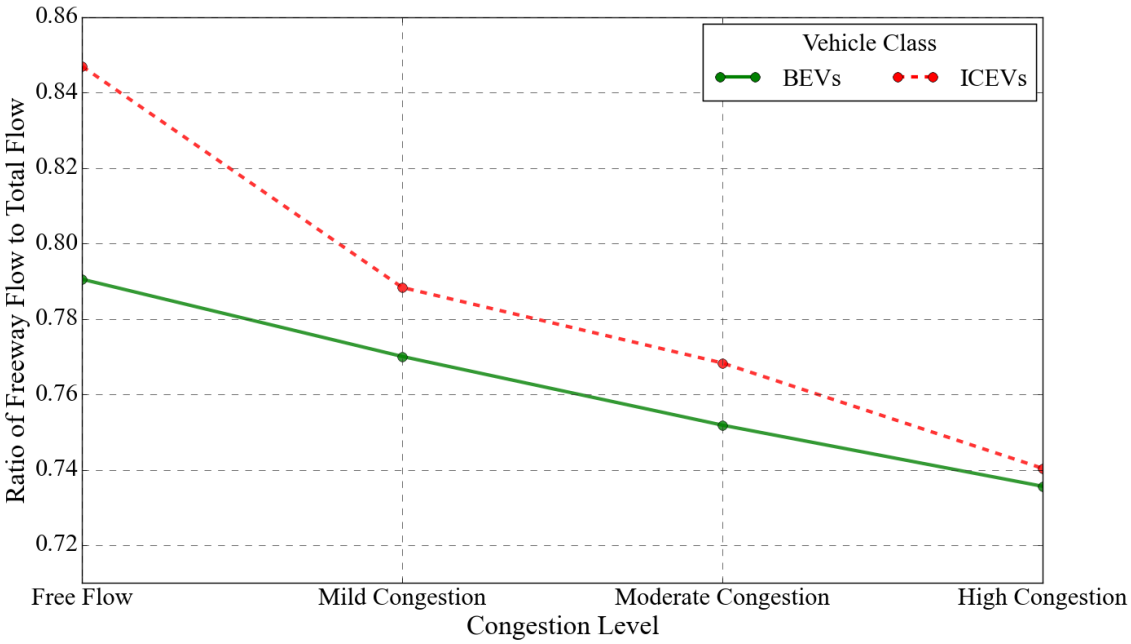

Figure 12 Effect of Congestion Level on Freeway Flow

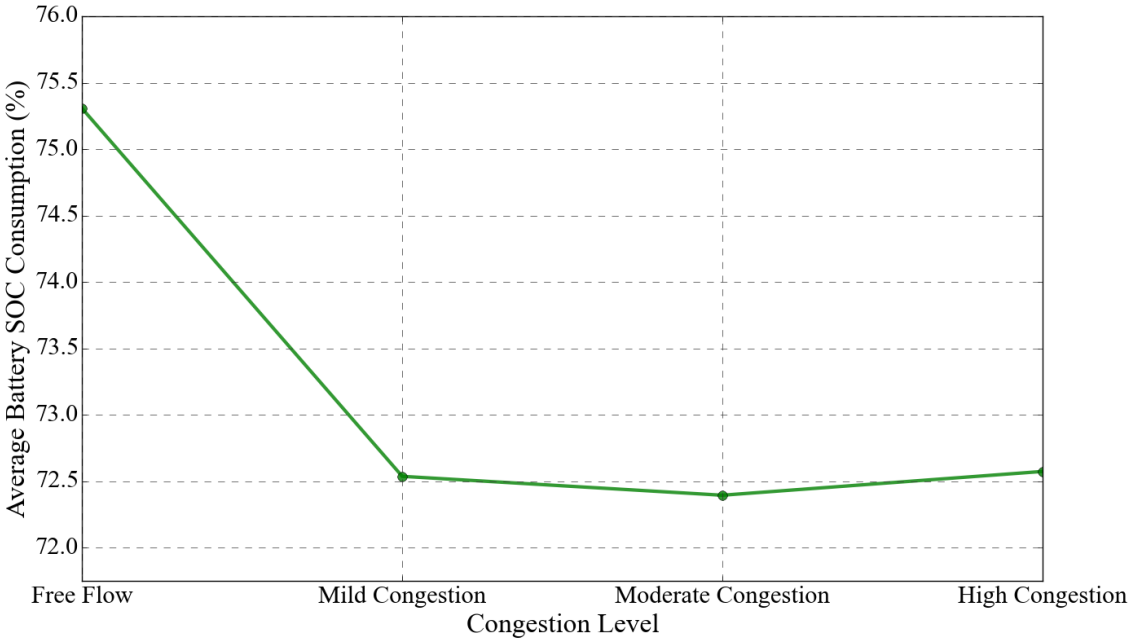

Figure 13 Effect of Congestion Level on Average Battery SOC Consumption

4.6. *Insights from Numerical Experiments*

The numerical experiments illustrate that, based on the generalized travel cost, BEV drivers in general tend to shift from the route with lower travel time (freeways) to routes with higher travel times (arterials) to reduce electricity costs and avoid range anxiety. This route choice aspect of

some BEVs reduces freeway congestion and benefits other vehicles using the freeway, but consequently increases congestion on arterial routes. The overall network performance is the net effect of these contrasting phenomena. In a network such as the one considered for the study experiments, where freeway flow is significantly higher than that of arterials, BEVs will have a positive impact on the overall network performance.

The route choice behavior tends to have a positive impact on overall system performance under both an increase in BEV market penetration and electricity cost. However, under very high BEV market penetration or at very high electricity cost, increased congestion on arterials more than negates the freeway benefits, leading to reduced system performance. The average battery SOC consumption of BEVs increases with their market penetration as more BEVs are on freeway, while it decreases with increase in electricity cost as they have more incentive to shift to arterial routes.

As traffic congestion increases, average network speed decreases, thereby reducing incentive for BEVs to select alternative routes to save on energy consumption. This increases the relative importance of travel time in the BEV route choice behavior, reducing the difference in route choice behavior of BEVs and ICEVs. The average battery SOC consumption decreases with increase in congestion until the moderate traffic congestion level. Under the high congestion level, the average battery SOC consumption increases as the vehicles travel a major portion of their trip at very low speeds (less than 10 mph) which is not energy-efficient for BEVs.

In summary, BEV route choice imperatives can synergistically lead to improved network performance under mixed traffic conditions for traffic networks with high levels of freeway flow and the availability route alternatives involving arterials.

5. Concluding Comments

This study analyzes the differences between the route choice behaviors of BEVs and ICEVs in a mixed traffic context with the potential for BEV range anxiety, and analyzes their implications for network performance under equilibrium conditions. A multi-class DUE model is formulated and a microscopic simulation-based solution procedure is proposed. The use of microscopic simulation as part of the solution procedure enhance the accuracy of BEV energy consumption computation. Consequently, it aids in realistically capturing the effect of traffic congestion on BEV route selection. The network performance in terms of travel time and energy consumption is analyzed with respect to network characteristics such as market penetration and congestion, and factors that affect BEV route choice such as electricity cost and range anxiety threshold.

As battery SOC consumption for BEVs is lower at slower speeds, they can reduce their energy consumption by traveling on routes with slower speeds. Moreover, the RBS system equipped in BEVs reduces the rate of energy dissipation in stop-and-go traffic conditions and makes it more economical for them in terms of battery SOC consumption. The results from the numerical experiments indicate that BEVs choose routes with slower speeds, typically arterial routes, to reduce their battery SOC consumption and avoid range anxiety. Such potential unconventional route choice behavior by BEVs based on generalized travel cost can decrease congestion on routes with higher free flow speeds while increasing congestion on routes with lower free flow speeds.

This can lead to the improvement of network performance and move the traffic network towards system optimal conditions in terms of travel time. Furthermore, with an increase in traffic congestion, BEV route choice behavior becomes similar to that of ICEVs as speeds in the network decrease, thereby reducing BEV incentive to switch routes to save on energy consumption.

In summary, this study investigates the impact of the increasing adoption of BEVs on traffic network performance. The numerical analysis provides useful insights related to BEV route choice behavior and its impact on network performance. These insights can aid traffic operators to devise control strategies in the emerging mixed traffic stream, and policy makers to determine an optimal trajectory for promoting electric vehicles. Further, the insights related to energy consumption can aid energy operators to plan for infrastructure investments to support the increasing market penetration of electric vehicles.

Acknowledgments

This study is based on research supported by the NEXTRANS Center, the USDOT Region 5 University Transportation Center at Purdue University. Any errors or omissions remain the sole responsibility of the authors.

References

Adler, J.D., Mirchandani, P.B., 2014. Online routing and battery reservations for electric vehicles with swappable batteries. Transportation Research Part B: Methodological 70, 285–302.

Adler, J.D., Mirchandani, P.B., Xue, G., Xia, M., 2014. The electric vehicle shortest-walk problem with battery exchanges. Networks and Spatial Economics 1–19.

Artmeier, A., Haselmayr, J., Leucker, M., Sachenbacher, M., 2010. The shortest path problem revisited: Optimal routing for electric vehicles, in: KI 2010: Advances in Artificial Intelligence. Springer, 309–316.

Astarita, V., 1996. A continuous time link model for dynamic network loading based on travel time function, in: Lesort, J.-B. (Ed.), Proceedings of the 13th International Symposium on Transportation and Traffic Theory. Pergamori, Oxford, 79–102.

Ban, X.J., Liu, H.X., Ferris, M.C., Ran, B., 2008. A link-node complementarity model and solution algorithm for dynamic user equilibria with exact flow propagations. Transportation Research Part B: Methodological 42, 823–842.

Barceló, J., Casas, J., 2005. Dynamic network simulation with AIMSUN, in: Simulation Approaches in Transportation Analysis. Springer, 57–98.

Becker, T.A., Sidhu, I., Tenderich, B., 2009. Electric vehicles in the United States: a new model with forecasts to 2030. Center for Entrepreneurship & Technology (CET) Technical Brief.

Blink, 2015. Car Charging Group, Inc. [ONLINE] Available at: http://www.blinknetwork.com [Accessed: 30 November 2015]

Botsford, C., Szczepanek, A., 2009. Fast charging vs. slow charging: Pros and cons for the new age of electric vehicles, in: EVS24 International Battery, Hybrid Fuel Cell Electric Vehicle Symposium.

Casas, J., Ferrer, J.L., Garcia, D., Perarnau, J., Torday, A., 2010. Traffic simulation with aimsun, in: Fundamentals of Traffic Simulation. Springer, 173–232.

Chabini, I., 1998. Discrete dynamic shortest path problems in transportation applications: Complexity and algorithms with optimal run time. Transportation Research Record: Journal of the Transportation Research Board 170–175.

Chan, H.L., 2000. A new battery model for use with battery energy storage systems and electric vehicles power systems, in: Power Engineering Society Winter Meeting, 2000. IEEE. 470–475.

Chen, T.D., Kockelman, K.M., Khan, M., others, 2013. The electric vehicle charging station location problem: a parking-based assignment method for Seattle, in: Transportation Research Board 92nd Annual Meeting. 13–1254.

CPLEX, IBM ILOG, 2012, V12. 5: User's manual for CPLEX

Haaren, R. Van, 2011. Assessment of electric cars' range requirements and usage patterns based on driving behavior recorded in the National Household Travel Survey of 2009. Earth and Environmental Engineering Department, Columbia University, Fu Foundation School of Engineering and Applied Science, New York.

He, F., Wu, D., Yin, Y., Guan, Y., 2013. Optimal deployment of public charging stations for plug-in hybrid electric vehicles. Transportation Research Part B: Methodological 47, 87–101.

He, F., Yin, Y., Lawphongpanich, S., 2014. Network equilibrium models with battery electric vehicles. Transportation Research Part B: Methodological 67, 306–319.

Hess, A., Malandrino, F., Reinhardt, M.B., Casetti, C., Hummel, K.A., Barceló-Ordinas, J.M., 2012. Optimal deployment of charging stations for electric vehicular networks, in: Proceedings of the First Workshop on Urban Networking. 1–6.

Ichimori, T., Ishii, H., Nishida, T., 1983. Two routing problems with the limitation of fuel. Discrete Applied Mathematics 6, 85–89.

Jiang, N., Xie, C., 2014. Computing and analyzing mixed equilibrium network flows with gasoline and electric vehicles. Computer-Aided Civil and Infrastructure Engineering 29, 626–641.

Jiang, N., Xie, C., Duthie, J.C., Waller, S.T., 2014. A network equilibrium analysis on destination, route and parking choices with mixed gasoline and electric vehicular flows. EURO Journal on Transportation and Logistics 3, 55–92.

Jiang, N., Xie, C., Waller, S., 2012. Path-constrained traffic assignment: model and algorithm. Transportation Research Record: Journal of the Transportation Research Board 25–33.

Johnson, V.H., 2002. Battery performance models in ADVISOR. Journal of Power Sources 110, 321–329.

Kuby, M., Lim, S., 2005. The flow-refueling location problem for alternative-fuel vehicles. Socio-Economic Planning Sciences 39, 125–145.

Maia, R., Silva, M., Araújo, R., Nunes, U., 2011. Electric vehicle simulator for energy consumption studies in electric mobility systems, in: Integrated and Sustainable Transportation System (FISTS), 2011 IEEE Forum on. 227–232.

Mak, H.-Y., Rong, Y., Shen, Z.-J.M., 2013. Infrastructure planning for electric vehicles with battery swapping. Management Science 59, 1557–1575.

Mock, P., Schmid, S.A., Friedrich, H.E., 2010. Market prospects of electric passenger vehicles, in: Electric and Hybrid Vehicles: Power Sources, Models, Sustainability, Infrastructure and the Market Elsevier, 545-577.

Mock, P., Yang, Z., 2014. Driving electrification: A global comparison of fiscal incentive policy for electric vehicles. The International Council on Clean Transportation (ICCT) 22, 2014.

Nie, Y.M., Ghamami, M., 2013. A corridor-centric approach to planning electric vehicle charging infrastructure. Transportation Research Part B: Methodological 57, 172–190.

NREL, 2013. ADVISOR Advanced Vehicle Simulator. [ONLINE] Available at: http://adv-vehicle-sim.sourceforge.net

Peeta, S., Ziliaskopoulos, A.K., 2001. Foundations of dynamic traffic assignment: The past, the present and the future. Networks and Spatial Economics 1, 233–265.

Plett, G.L., 2004. Extended Kalman filtering for battery management systems of LiPB-based HEV battery packs: Part 3. State and parameter estimation. Journal of Power Sources 134, 277–292.

Rezvanizaniani, S.M., Liu, Z., Chen, Y., Lee, J., 2014. Review and recent advances in battery health monitoring and prognostics technologies for electric vehicle (EV) safety and mobility. Journal of Power Sources 256, 110–124.

Sachenbacher, M., Leucker, M., Artmeier, A., Haselmayr, J., 2011. Efficient energy-optimal routing for electric vehicles, in: Twenty-Fifth AAAI Conference on Artificial Intelligence.

Schneider, M., Stenger, A., Goeke, D., 2014. The electric vehicle-routing problem with time windows and recharging stations. Transportation Science 48, 500–520.

Senart, A., Kurth, S., Le Roux, G., 2010. Assessment framework of plug-in electric vehicles strategies, in: Smart Grid Communications (SmartGridComm), 2010 First IEEE International Conference on. 155–160.

Shepherd, S., Bonsall, P., Harrison, G., 2012. Factors affecting future demand for electric vehicles: A model based study. Transport Policy 20, 62–74.

Smith, M.J., 1984. The stability of a dynamic model of traffic assignment-an application of a method of Lyapunov. Transportation Science 18, 245–252.

Storandt, S., 2012. Quick and energy-efficient routes: computing constrained shortest paths for electric vehicles, in: Proceedings of the 5th ACM SIGSPATIAL International Workshop on Computational Transportation Science. 20–25.

Straubel, J.B., 2008. Roadster efficiency and range. Tesla Motors 22.

Tanaka, D., Ashida, T., Minami, S., 2008. An analytical method of EV velocity profile determination from the power consumption of electric vehicles, in: Vehicle Power and Propulsion Conference, 2008. VPPC'08. IEEE. 1–3.

Tate, E.D., Harpster, M.O., Savagian, P.J., 2008. The electrification of the automobile: from conventional hybrid, to plug-in hybrids, to extended-range electric vehicles. SAE International Journal of Passenger Cars-Electronic and Electrical Systems 1, 156–166.

Upchurch, C., Kuby, M., Lim, S., 2009. A model for location of capacitated alternative-fuel stations. Geographical Analysis 41, 85–106.

USDOE, 2015. All-electric vehicles. [ONLINE] Available at: http://www.fueleconomy.gov/feg/evtech.shtml

USDOE, 2014. Benefits and considerations of electricity as a vehicle fuel. [ONLINE] Available at: http://www.afdc.energy.gov/fuels/electricity_benefits.html

Wang, Y.-W., Lin, C.-C., 2009. Locating road-vehicle refueling stations. Transportation Research Part E: Logistics and Transportation Review 45, 821–829.

Wipke, K.B., Cuddy, M.R., Burch, S.D., 1999. ADVISOR 2.1: A user-friendly advanced powertrain simulation using a combined backward/forward approach. Vehicular Technology, IEEE Transactions on 48, 1751–1761.

Wu, X., Freese, D., Cabrera, A., Kitch, W.A., 2015. Electric vehicles' energy consumption measurement and estimation. Transportation Research Part D: Transport and Environment 34, 52–67.

Xi, X., Sioshansi, R., Marano, V., 2013. Simulation-optimization model for location of a public electric vehicle charging infrastructure. Transportation Research Part D: Transport and Environment 22, 60–69.

Xie, C., Jiang, N., 2016. Relay requirement and traffic assignment of electric vehicles. Computer-Aided Civil and Infrastructure Engineering. doi: 10.1111/mice.12193

Yao, E., Wang, M., Song, Y., Yang, Y., 2013. State of charge estimation based on microscopic driving parameters for electric vehicle's battery. Mathematical Problems in Engineering 2013.

Yu, A.S.O., Silva, L.L.C., Chu, C.L., Nascimento, P.T.S., Camargo Jr, A.S., 2011. Electric vehicles: struggles in creating a market, in: Technology Management in the Energy Smart World (PICMET), 2011 Proceedings of PICMET'11: 1–13.